

Seismo-acoustic analysis of the infrasound events on 2010, February 03

Láslo G. Evers

KNMI technical report = technisch rapport; TR-3 14

De Bilt, 2010

PO Box 201
3730 AE De Bilt
Wilhelminalaan 10
De Bilt
The Netherlands
<http://www.knmi.nl>
Telephone +31(0)30-220 69 11
Telefax +31(0)30-221 04 07

Author: Evers, L.G.



Contents

1	Introduction	1
2	Observations and data processing	3
2.1	Infrasound recordings at the Texel Infrasound Array (TEX)	3
2.1.1	Observations	3
2.1.2	Processing of infrasound array data	4
2.2	Recording at the seismic borehole station near Firdgum (FDG)	7
2.2.1	Observations	7
2.2.2	Waveform characteristics	7
2.3	Summary and source identification	9
3	Infrasound propagation through the atmosphere	11
3.1	The influence of wind and temperature	11
3.2	Raytracing to analyze the infrasound propagation	12
3.2.1	Direct propagation to TEX	13
3.2.2	Refractive propagation to FDG	13
3.3	Amplitude considerations	14
4	Discussion	15
5	Conclusions	17
A	Press release	19
	Bibliography	20
	Summary	23
	Samenvatting	25
	Acknowledgments	27

Introduction

The Seismology Division of the Koninklijk Nederlands Meteorologisch Instituut (KNMI) operates a network of seismic and acoustic sensors in the Netherlands. Information on vibrations is provided to the Dutch society on the basis of signals detected by this network. The main causes of vibrations are earthquakes and low frequency acoustic waves, i.e., infrasound, in the atmosphere. The latter can be generated by shock waves associated with for example explosions and supersonic flying. By monitoring both the solid earth and the atmosphere, a distinction can be made between the causes of vibrations which enhances the capability to identify the sources.

Vibrations were reported by citizens of Friesland on 2010, February 03. This province has recently gained seismological attention because of its citizen who felt vibrations and associated those with subsurface salt explorations. A network of borehole seismometers is currently being realized to monitor the possible occurrence of earthquakes. In this report, measurements from one of these borehole seismometers near Firdgum will be used (see Figure 1.1) in analyzing the possible cause of the reported vibrations on February 03. Such a borehole setup consists of four levels, separated by 30 meters, equipped with three-component geophones. Infrasound measurements near Friesland are conducted at the island of Texel with a six element microbarometer array (see Figure 1.1). A microbarometer is sensitive to infrasound within the frequency range of 0.002 to 20 Hz. An analog noise reducer is connected to each microbarometer to reduce the effect of wind noise on the measurements [Evers, 2008].

The aim of this report is to identify the source of the reported vibrations based on observations of atmospheric pressure variations. Furthermore, attention will be paid to wave propagation through a dynamic atmosphere.

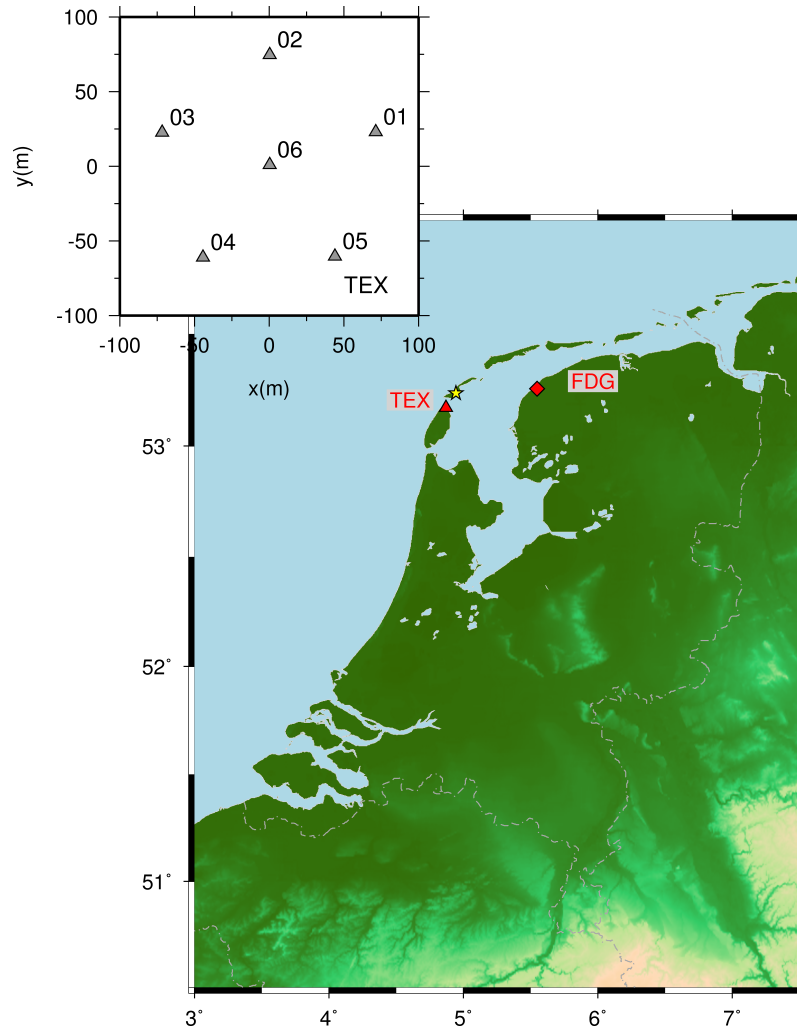


Figure 1.1: Map of the Netherlands showing the location of the Texel Infrasound Array (TEX) and the borehole seismometer near Firdgum (FDG). The layout of TEX is shown in the inlay. The yellow star indicates the Vliehors on the island of Vlieland.

Observations and data processing

2.1 Infrasound recordings at the Texel Infrasound Array (TEX)

■ 2.1.1 Observations

Infrasound is being measured by TEX 24 hours per day. The lower frame of Figure 2.1 shows the result of such a measurement on 2010, February 03 at microbarometer 01 (see Figure 1.1). There is a significant amount of high frequency noise superimposed on the background air pressure fluctuations. These rapid fluctuations are caused by wind in the lower atmosphere, i.e., the boundary layer, and have amplitudes between -10 and 10 Pa. From 16h30 and onwards, these fluctuations decrease in intensity and amplitude,

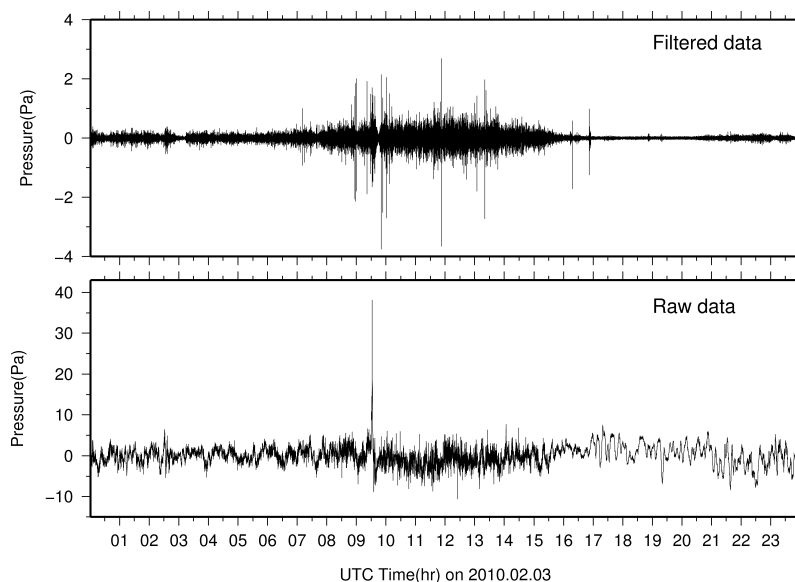


Figure 2.1: Recording of microbarometer 01 (see Figure 1.1) of TEX. The lower frame gives the unfiltered measurement of air pressure on 2010, February 03. The recording shown in the top frame is band-pass filtered with a second order Butterworth filter having corner frequencies of 1.0 and 9.0 Hz.

Table 2.1: Summary of observations and processing results of TEX

UTC time (hh:mm:ss)	Amp- litude(Pa)	Back azimuth(deg)	Apparent sound speed(m/s)	Fisher ratio
08:57:29	4.0	36.5	342.7	7.0
08:58:15	4.7	39.0	362.7	5.5
09:00:19	4.8	39.0	362.7	5.3
09:22:07	4.5	39.0	362.7	6.6
09:29:33	3.8	39.0	362.7	6.1
09:51:17	5.3	39.0	362.7	5.6
09:54:06	4.1	38.3	404.8	7.6
10:01:17	5.7	39.0	362.7	6.2
10:07:34	4.0	39.0	362.7	4.8
11:52:56	6.8	39.0	362.7	4.9
13:05:05	3.8	39.0	362.7	5.8
13:21:12	4.7	39.0	362.7	8.0

which indicates a decrease in wind speeds.

A strong impulsive event is visible around 9h30 with a long period tail of approximately 500 s. This wave is a density current that travels with wind speed like velocities over the array. In other words, the density current is a non-acoustic atmospheric wave.

The top frame of Figure 2.1 shows the band-pass filtered recording of microbarometer 01. A second order Butterworth band-pass filter has been applied with corner frequencies at 1.0 and 9.0 Hz. Clearly, the noise due to wind is strongest during daytime (UTC+1h) and diminishes after 16h30. Furthermore, a series of impulsive events are visible during the day with amplitudes up to 4 Pa.

■ 2.1.2 Processing of infrasound array data

A detection algorithm is applied to the recordings of TEX to extract events of interest. Such an algorithm evaluates the signal coherency of waves traveling over the array. In this case, detection is realized by evaluating the Fisher statistics which is a measure of signal-to-noise ratio (SNR). If an event is detected, its parameters are estimated through beamforming. The process of beamforming evaluates the traveltimes differences over the array in order to find the back azimuth and apparent sound speed of the wave. The back azimuth is the clockwise angle measured from the north, indicating the direction where the energy comes from. The apparent sound speed is the propagation velocity of the wave over the array as measured by the microbarometers, i.e., the horizontal component of the propagation velocity. A detailed description of the above processing scheme can be found in *Evers* [2008].

Figure 2.2 shows the recordings from the microbarometers of TEX between 08h55m00s and 09h01m40s. Three impulsive events are clearly recorded by all sensors. The noise levels, due to winds, strongly vary over the array. Especially, microbarometer 05 and 06 show a large amount of incoherent air pressure fluctuations. In addition to wind, such variations can be caused by a degradation of the analog noise reducers which are connected to each sensor. A similar effect causes microbarometer 04 to be less sensitive. Nevertheless, the three coherent events can easily be distinguished from the background noise and might each find their origin at one specific source. Array processing techniques are applied to further investigate the coherent arrivals. Figure 2.3 shows the results of such an analysis. For each event, a significant increase in the Fisher ratio (or SNR^2) is obtained from the coherency analysis as shown in the lower frame. The middle two frames show the calculated apparent sound speed and back azimuth. Values close to the sound speed are resolved (see the red dots) indicating that an infrasound wave traveled over the array. The back azimuth points

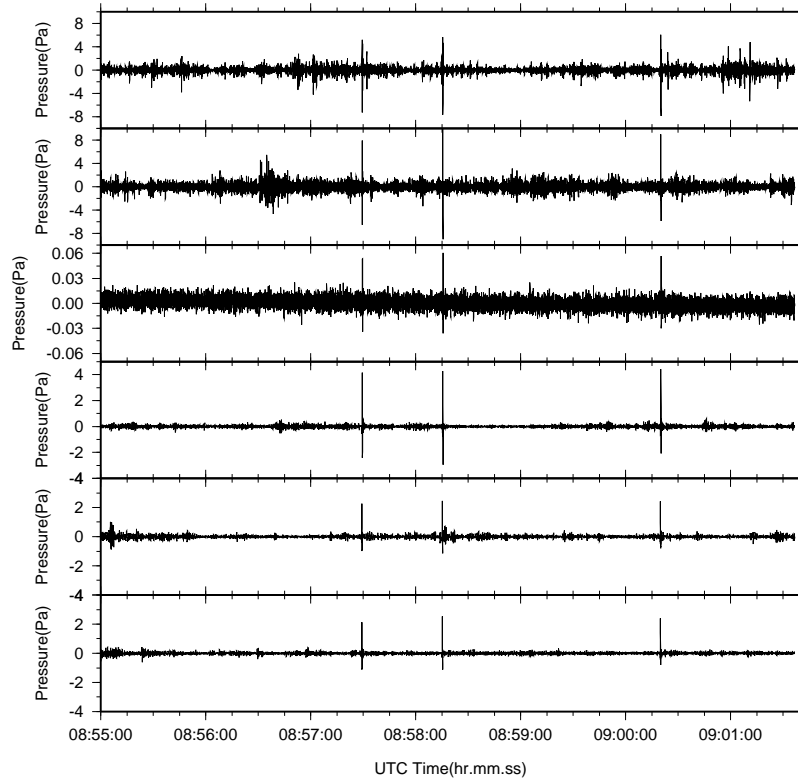


Figure 2.2: The recordings of TEX made between 08h55m00s and 09h01m40s, band-pass filtered between 1.0 and 9.0 Hz. Data from microbarometer 01 up to 06 are shown, respectively, from bottom to top. Although the noise levels and amplitudes highly differ at each microbarometer, three impulsive events should be noted on all microbarometers.

to a northeastern direction for the source, i.e., between 36.5 and 39 deg. The top frames show the best beam which is the sum of the phase aligned individual recordings and a spectrogram based on a sliding window Fast Fourier Transform (FFT) [Press *et al.*, 1992]. The peak frequency of the events is 3.8 Hz. The waveforms have a typical blastwave signature indicative for a nearby explosion.

By applying the above analysis to data from the whole day of February 3, a total of 12 coherent infrasound waves have been detected at TEX. These waves all appeared from the northeast, their characteristics are given in Table 2.1. The apparent sound speed is somewhat higher than the sound speed, this indicates a slight vertical component to the incidence angle of the wave. In other words, the wave does not travel parallel to the earth's surface but has slight curvature. This can probably be explained by the dike around Texel which requires a elevated propagation path of the infrasound wave to pass over and reach the array.

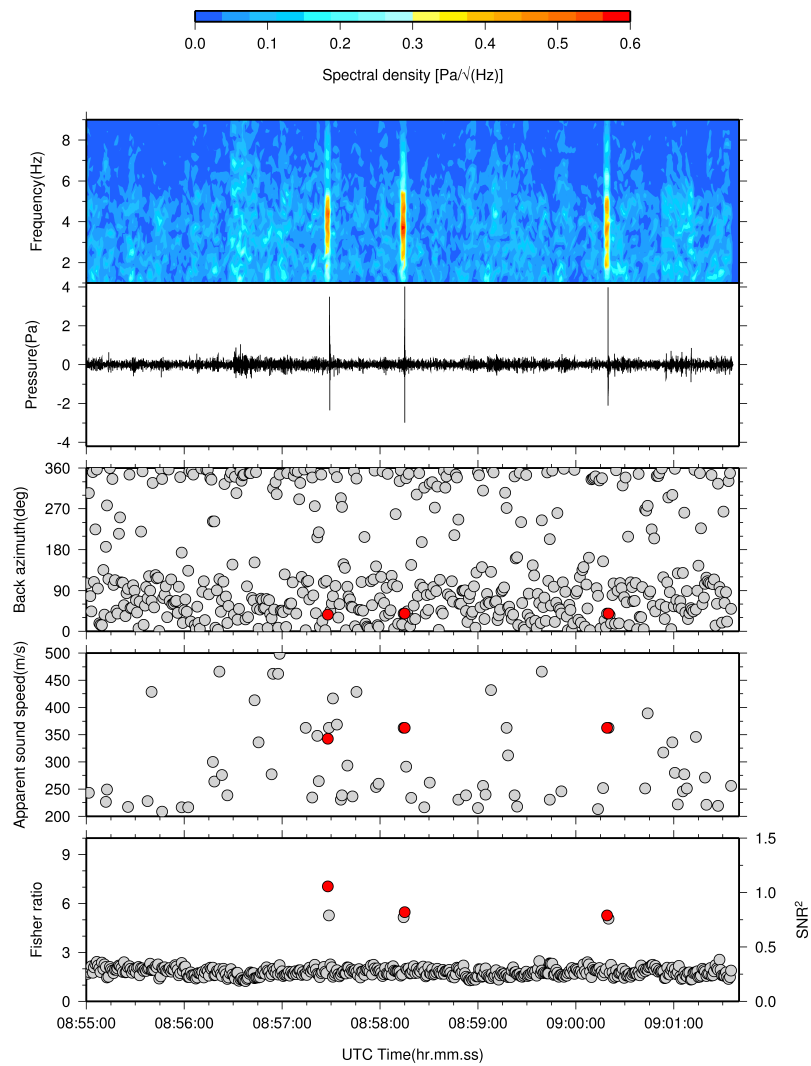


Figure 2.3: Results of the array processing of TEX infrasound data between 08h55m00s and 09h01m40s. The lower frame shows the Fisher ratio or signal-to-noise power ratio (SNR^2) as function of time. The two middle frames show the resolved apparent sound speed and back azimuth. The top frames show the best beam, i.e., the sum of the time aligned individual microbarometer recordings and its spectrogram. Events of interest are given by the red dots and correspond to the sharp peaks in the best beam and high spectral densities.

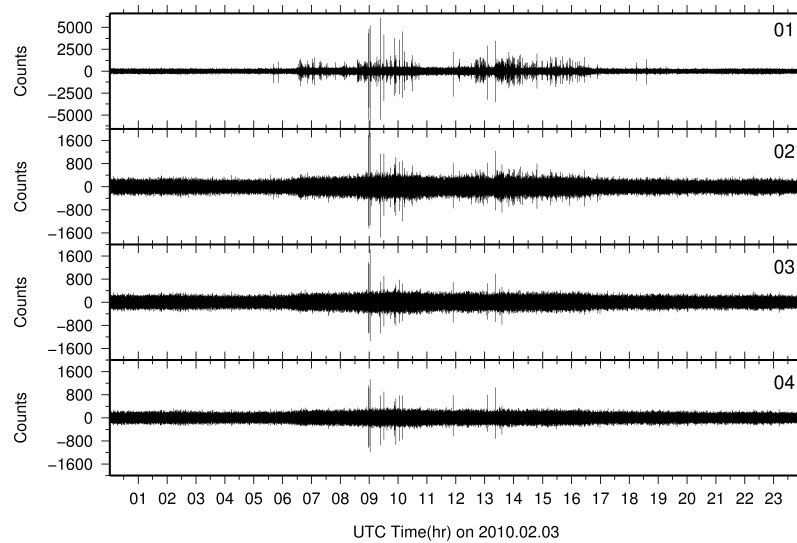


Figure 2.4: Recordings of the borehole seismic station near Firdgum (FDG) on 2010, February 03. The vertical components of the ground movement are shown at level 01, 02, 03 and 04, which corresponds to depths of 30, 60, 90 and 120 m, respectively. The recordings are band-pass filtered between 1.0 and 9.0 Hz with a second order Butterworth filter. Note the different scales used for the first level and subsequent levels.

2.2 Recording at the seismic borehole station near Firdgum (FDG)

■ 2.2.1 Observations

The solid earth is monitored with a network of borehole seismic station in the north of the Netherlands. Figure 2.4 shows the recordings made near Firdgum (Friesland) on 2010, February 03. The seismic traces are taken from the vertical component of the three-component geophones. These are located at depths of 30 m (level 01), 60 m (02), 90 m (03) and 120 m (04), respectively.

Several impulsive events are present in the recordings during daytime. The events are most pronounced at the first level but also leave their signature at larger depths (note the difference in scales in Figure 2.4). Such a behavior is indicative for an atmospheric acoustic wave, where the amplitude decreases with depth. In case of an earthquake, such an amplitude decrease wouldn't be observed from a source at depth.

Since three-component geophones are used, the particle motion can be analyzed. Such an analysis indicates from which direction the energy arrives at the sensor. The average direction is $266 \pm 10^\circ$ which point towards an area near Texel and Vlieland. This average is based on 11 events; from one event the *SNR* was too low prohibiting such an analysis.

■ 2.2.2 Waveform characteristics

The 12 events as identified in the TEX recordings are also measured by FDG. Figure 2.5 gives an example of such a recording. The arrival time, amplitude and period are picked for all events and listed in Table 2.2. These values are taken from the vertical component of the geophone at the first level. The velocity derived from the amplitude and period is also given in Table 2.2. This velocity is called the peak ground velocity and represents the velocity with which the particles move in the subsurface near the sensor. These values also indicate that the vibrations are caused by infrasound in the atmosphere since ground velocities in order of 10^{-6} m/s are not felt by humans (values of 10^{-2} m/s and higher are sensed, typically).

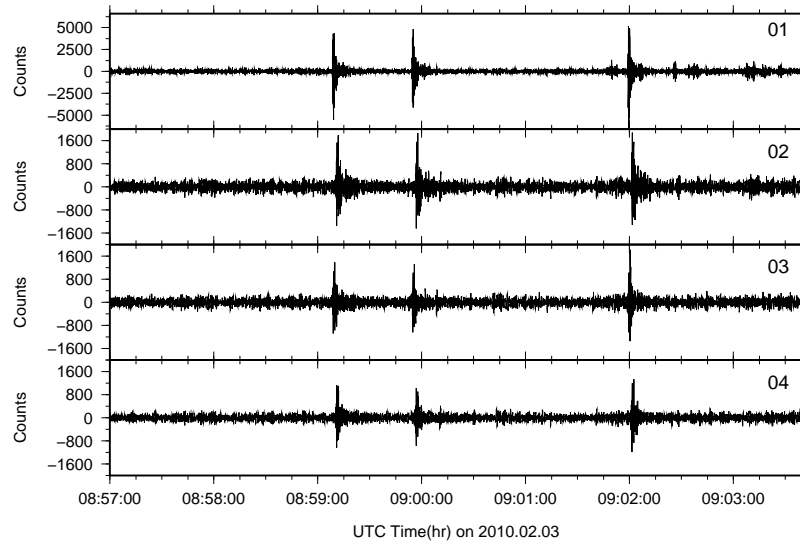


Figure 2.5: Recordings of the borehole seismic station FDG between 08h57m00s and 09h03m40s, following the same convention in order as used in Figure 2.4.

Table 2.2: Summary of observations at FDG

UTC time (hh:mm:ss)	Amp- litude(nm)	Period (s)	Peak ground velocity (10^{-6} m/s)
08:59:09	404	0.23	1.8
08:59:55	524	0.25	2.1
09:01:59	676	0.26	2.6
09:23:47	551	0.23	2.4
09:31:13	466	0.23	2.0
09:52:56	229	0.19	1.2
09:55:45	200	0.19	1.1
10:02:56	360	0.24	1.5
10:09:14	224	0.21	1.1
11:54:36	222	0.18	1.2
13:06:43	181	0.15	1.2
13:22:53	259	0.15	1.7

2.3 Summary and source identification

Infrasound waves have been detected in both TEX and FDG. A source location to the northeast of TEX indicates possible activity at Vliehors (Vlieland) as also derived from the particle motion in FDG. There is a consistent traveltime difference between TEX and FDG of 100 s. This also points to a source location in the area of the Vliehors. Personal communication with the Ministry of Defense has revealed that an exercise took place on 2010, February 03. This exercise was also announced in a press release (see Appendix A) for the period of February 01 up to 05. A total of 12 bombs (type: MK-82 500 pounds) have been thrown from F-16 fighters near $53.23694^{\circ}\text{N}, 4.94389^{\circ}\text{E}$ (see the yellow star in Figure 1.1).

Infrasound propagation through the atmosphere

This chapter describes the propagation of infrasound through the dynamic atmosphere. A detailed modeling will be conducted to understand how the energy traveled, from the Vliehors to TEX and FDG, under the influence of the wind and temperature within the troposphere, i.e., the first 10 km of the atmosphere.

3.1 The influence of wind and temperature

Infrasound wave propagation is, in first order, dependent on the composition, wind and temperature structure of the atmosphere. The effective sound speed incorporates these effects and is described by e.g. *Gossard and*

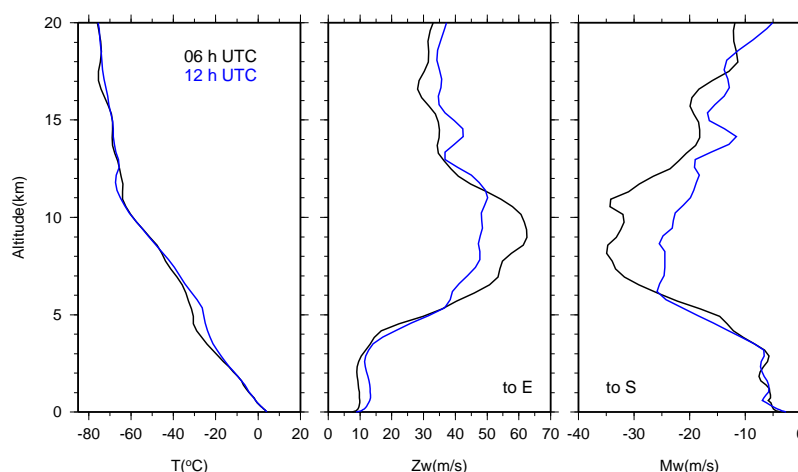


Figure 3.1: Temperature and wind from the ECMWF analysis valid for 06h (in black) and 12h (in blue) UTC on 2010, February 03. Such models are available on a 0.5° by 0.5° grid. A grid node in between TEX and FDG is chosen at 53° N, 5° E. The middle frame gives the zonal wind, the right frame the meridional wind. These wind components have positive values when directed to the east and north, respectively.

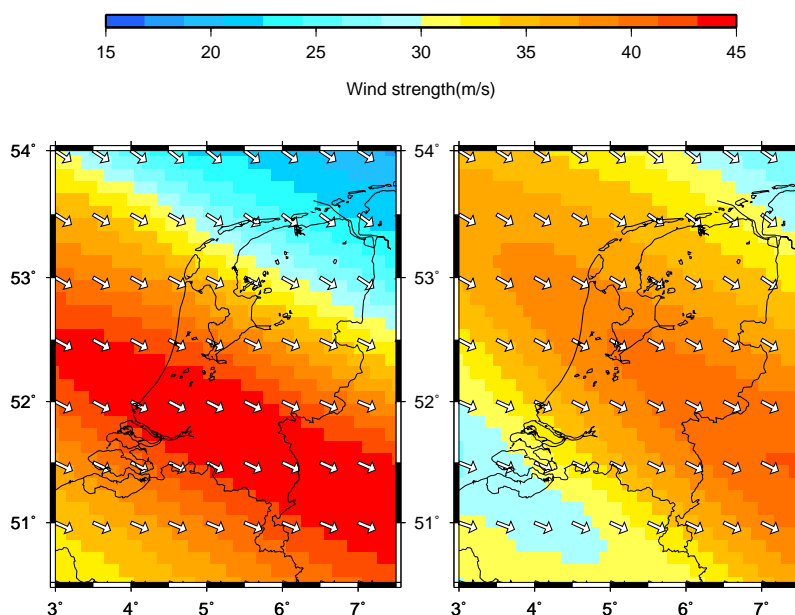


Figure 3.2: The wind strength and direction at an altitude of 5 km from the ECMWF analysis, for 06h UTC (left) and 12h UTC (right).

Hooke [1975]:

$$c_{eff} = \sqrt{\gamma_g RT} + \hat{n} \cdot \vec{u} = c_T + \hat{n} \cdot \vec{u} \quad (3.1.1)$$

where the multiplication of the ratio of specific heats, γ_g , with the gas constant for air, R , is $\gamma_g R = 402.8 \text{ m}^2 \text{ s}^{-2} \text{ K}^{-1}$. The absolute temperature is given by T and $\hat{n} \cdot \vec{u}$ projects the wind \vec{u} in the direction from source to observer \hat{n} , c_T is called the sound speed.

The temperature decreases with altitude in the lower atmosphere, under regular atmospheric circumstances. As a result of this, sound bends upward as function of horizontal distance. Refraction of infrasound back to the surface may occur from regions where c_{eff} becomes larger than its surface value. This can be caused by an increase in wind or temperature or a combined effect and follows from Snell's law.

The analysis of the wind and temperature structure of the atmosphere is provided by the European Centre for Medium-Range Weather Forecasts (ECMWF). Atmospheric models are provided every six hours (00h, 06h, 12h and 18h UTC) on a 0.5° by 0.5° grid. Such a model consists of 90 levels which covers an altitude range up to 80 km. The wind and temperature at $53^\circ \text{N}, 5^\circ \text{E}$ for 06h and 12h UTC are shown in Figure 3.1. The wind is split in a zonal (Zw) and meridional (Mw) component. The zonal wind has a positive sign when directed to the east, i.e., a westerly wind. A southerly wind has a positive sign for the meridional wind. Clearly, there is a strong gradient in the wind from 5 km altitude up to 10 km which will influence the infrasound propagation. This so-called jet stream is directed to the east with a slight component to the south. (see Figure 3.2). The temperature shows a regular decrease with altitude.

3.2 Raytracing to analyze the infrasound propagation

Raytracing is a computationally efficient way to analyze the propagation of infrasound through the atmosphere, taking into account the influence of wind and temperature [Garcés *et al.*, 1998]. Raytracing is a high frequency approach where it is assumed that a wave travels along a raytrajectory through the atmosphere. Such raytrajectories can be generated between the source and receiver with an assumed source location.

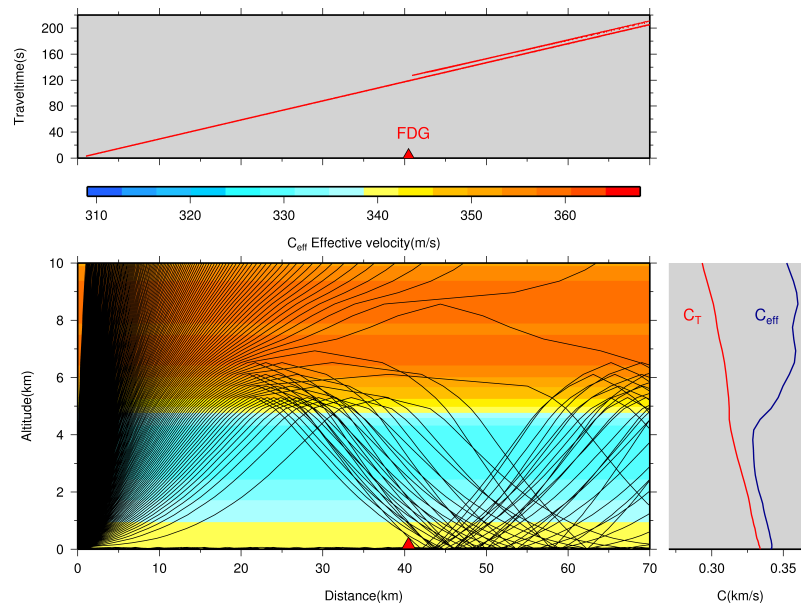


Figure 3.3: The propagation of infrasound from the Vliehors to FDG through the 06h UTC model at $53^{\circ}N, 5^{\circ}E$. The lower frame shows the raytrajectories for energy leaving the source towards FDG. The frame to right gives the effective sound speed (c_{eff}) and sound speed (c_T). The top frame shows the traveltime for rays impinging on the earth's surface.

■ 3.2.1 Direct propagation to TEX

A source location of $53.23694^{\circ}N, 4.94389^{\circ}E$ was obtained from the Ministry of Defense, which means a source receiver distance to TEX of 8.8 km and back azimuth of 33.5 deg. The average wind in the lower atmosphere was directed to the east (280 deg) with velocities ranging between 6 and 10 m/s. This means that the energy traveled directly and upwind from the Vliehors towards TEX. The average observed back azimuth is 38.7 deg which makes an azimuthal deviation, i.e., the difference between the true and observed back azimuth, of -5.2 deg. Such a deviation is well explained by a westerly cross wind acting on the wavefront during its propagation from source to receiver.

■ 3.2.2 Refractive propagation to FDG

The source receiver characteristics for FDG are a distance of 40.5 km and back azimuth of 267.1 deg. Figure 3.3 shows how the energy propagates from the Vliehors to FDG through the 06h UTC model at $53^{\circ}N, 5^{\circ}E$. Refractions back to the earth's surface occur from an altitude of 5 km. At this altitude the effective sound speed (c_{eff}) becomes larger than its surface value. The wind is responsible for this so-called waveguide. For comparison, c_{eff} and the sound speed (c_T), i.e., without wind, are plotted in the frame to the right. FDG appears to be located just at the edge of the shadow zone for the first jet stream returns.

From the traveltime curves it follows that there is a small surface waveguide, filling up shadow zone with arrivals. The corresponding raytrajectories are hardly visible in the lower frame because the waveguide has a thickness of less than 50 m. The first jet stream arrivals to appear at FDG have traveled for 126 s.

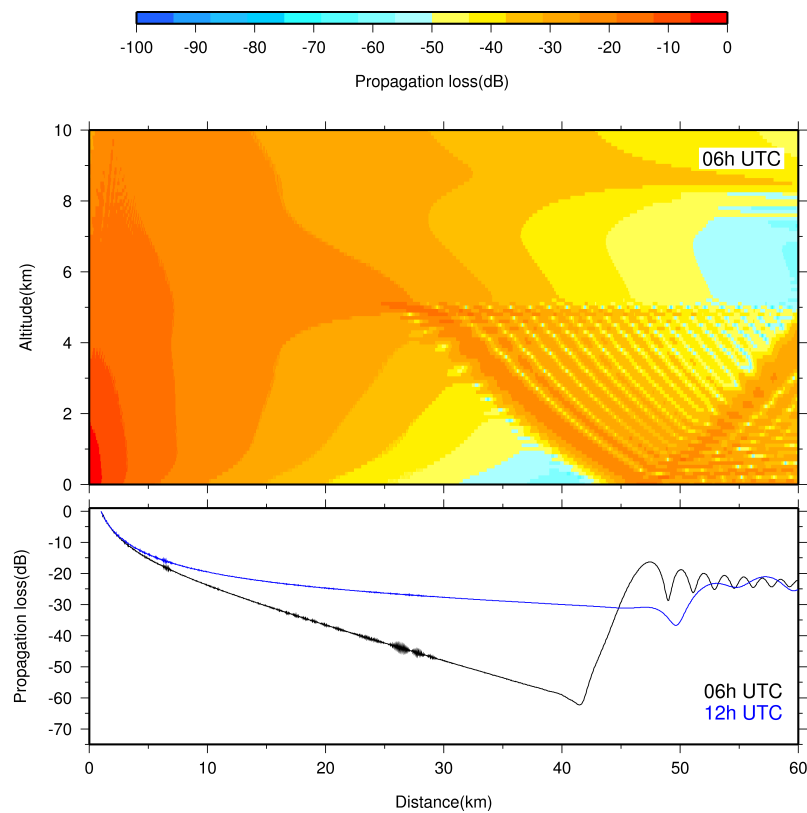


Figure 3.4: The intrinsic loss of infrasound due to molecular relaxation of the infrasonic energy of 5 Hz. The propagation is valid for the trajectory Vliehors-FDG. The upper frame shows the loss for the 06h UTC model. The lower frame shows the loss as notable on the earth's surface, i.e., at an altitude of zero km, for the 06h (in black) and 12h UTC (in blue) model.

3.3 Amplitude considerations

In this section, an example of amplitude modeling is given which should currently be labeled as work in progress at the author's institute. Figure 3.4 shows the intrinsic loss of infrasound energy as a function of altitude and distance. This loss is valid for the propagation from the Vliehors to FDG. Such loss calculations are based on the parabolic equation approximation as described by *Lingevitch et al.* [2002]. The amount of loss is controlled by the molecular relaxation of the infrasound wave passing through the mixed gas, i.e., air [*Sutherland and Bass*, 2004]. In addition, to this loss the geometrical spreading has to be taken into account which will considerably increase the total loss. If such refinements to the modeling are realized, its output should be validated with infrasound array measurements at various source-receiver distances.

Discussion

The wind conditions on 2010, February 03 were favorable for propagation of the infrasound from the Vliehors towards Friesland. The question now arises how unique the occurrence of such winds is. Figure 4.1 shows the wind gradients for a year of atmospheric models provided by the ECMWF. The wind gradient between an altitude of 5 and 10 km is calculated from 6-hourly models at the location $53^{\circ}\text{N}, 5^{\circ}\text{E}$. The gradient was $3.4 \text{ m}(\text{s km})^{-1}$ and $7.4 \text{ m}(\text{s km})^{-1}$ on February 03 at 06 and 12 UT, respectively. Figure 4.1 also shows the wind direction; a value of 297 degrees was valid for February 03. The yellow area in the top frame represents a range of 297 ± 15 degrees. The green dots in the lower frame shows the occurrence of conditions similar to those on February 03, i.e., a gradient larger than $3.4 \text{ m}(\text{s km})^{-1}$ and wind direction of 297 ± 15 degrees. These conditions occur 5% of the time of the full year analyzed.

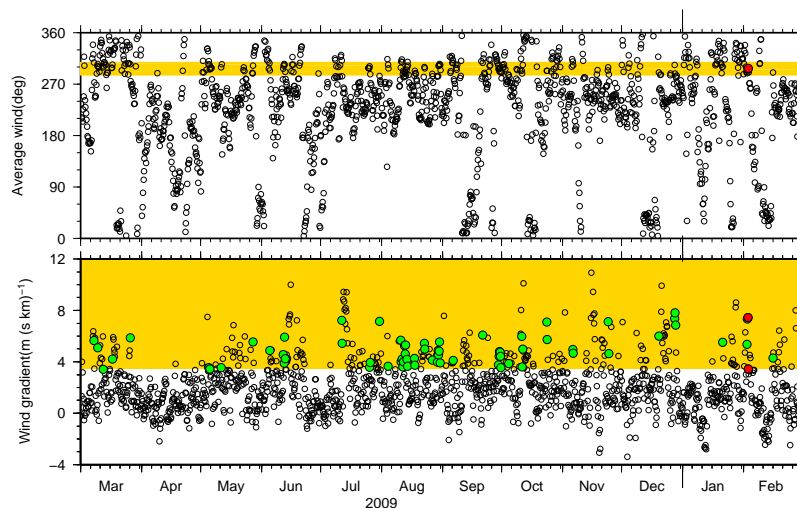


Figure 4.1: The wind gradient between the altitudes of 5 and 10 km (lower frame) from the ECMWF analysis at $53^{\circ}\text{N}, 5^{\circ}\text{E}$, and the values for 2010, February 03 as red dots. The yellow area indicated values higher than $3.4 \text{ m}(\text{s km})^{-1}$, i.e., the value at 12 UT on February 03. The top frame gives the average wind direction between 5 and 10 km. The yellow area indicates the direction on February 03 ± 15 degrees which is a direction from the Vliehors to Friesland. The green dots in the lower frame are values larger than $3.4 \text{ m}(\text{s km})^{-1}$ with a wind direction in the Vliehors-Friesland range.

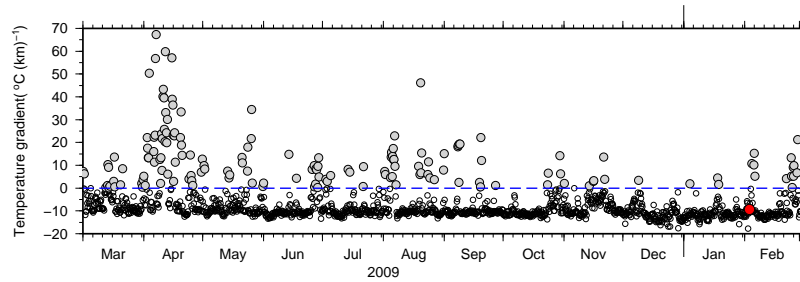


Figure 4.2: The occurrence of temperature inversions derived from the 6-hourly ECMWF analysis at $53^{\circ}N, 5^{\circ}E$. A positive temperature gradient represents an inversion in the first 100 m of the atmosphere. The red dots are valid for 2010, February 03.

Temperature inversions can also efficiently duct the infrasonic energy. Especially, propagation from the Vliehors towards Texel will be affected by such inversions and might cause vibrations on Texel. Figure 4.2 shows the occurrence of temperature inversions for a full year of ECMWF analysis at $53^{\circ}N, 5^{\circ}E$. Temperature inversions are present in case of a positive temperature gradient and are derived for the first 100 m of the atmosphere. Inversions occur 11% of the time.

Conclusions

Vibrations and damage, to for example infrastructure, can be caused by earthquakes and infrasound. The KNMI operates a network of seismic and infrasound sensors in the Netherlands to identify the sources. A total of 12 events have been detected by part of this network on 2010, February 03. Signals were recorded on a borehole seismometer (FDG) near Firdgum (Friesland) and an infrasound array (TEX) on Texel. Based on the signal characteristics, it was derived that these events were associated to an atmospheric source near Vlieland. A military exercise on the Vliehors (Vlieland) has been confirmed by the Ministry of Defense. The existence of this atmospheric source of infrasound was revealed by determining the arrival time, back azimuth and shape of the acoustic waves at TEX and FDG. The seismic particle motion, on the latter, also pointed to the Vliehors.

There are various ways in which infrasound waves can be efficiently channeled by the atmosphere over long ranges with a low attenuation. These are temperature inversions, strong surface down winds or strong wind jets higher up in the atmosphere. In this case, the explanation for the reported vibrations over ranges of 40 km and more were found in a strong down wind between 5 and 10 km altitude ranging from 10 to 60 m/s. This wind formed a favorable duct for infrasound propagation from the Vliehors to Friesland. These wind conditions are not unique but appear 5% of the time as follows from the analysis of a year of atmospheric specifications.

The modeling of infrasound amplitudes can be used to predict amplitudes over a variety of source-receiver distances. Such modeling should include the actual meteorological specifications for wind and temperature, as exemplified in this report. To accurately forecast the occurrence of certain sound pressure levels, validation of the model with infrasound measurements is required.

Press release

Persbericht

Datum 13 januari 2010
Ons kenmerk LW 2010/02



Ministerie van Defensie

Commando
Luchtstrijdkrachten
Vliegbasis Leeuwarden
Staf Voorlichting

Bezoekadres:
Vliegbasis Leeuwarden
Keegsdijkje 7
Postadres:
MPC 80 A
Postbus 21050
8900 JB Leeuwarden
Telefoon (058) 234 67 00
Fax (058) 234 63 99
www.luchtmacht.nl

Live weapons op de Vliehors Range

F-16 jachtvliegtuigen oefenen op maandag 1 februari tot en met vrijdagochtend 5 februari 2010 in het afwerpen van bommen met explosieve lading op de NAVO oefenlocatie de Vliehors Range op Vlieland. In totaal worden naar verwachting 16 bommen van het type MK82 (500 ponders) afgeworpen.

Bij deze trainingsvluchten richt het Bureau Geluidshinder van de Koninklijke Luchtmacht op Texel meetposten in, waarbij de geconstateerde weersomstandigheden en de daaruit voortvloeiende geluidsbelasting bepalend zijn voor het kunnen uitvoeren van de geplande oefeningen. Deze mobiele meetposten staan in direct contact met de verkeerstoren van de Vliehors Range.

Tijdens de oefeningen is de Vliehors Range op Vlieland voor publiek gesloten. De grens van het oefenterrein is gemarkeerd met waarschuwborden en bij oefening voorzien van rode vlaggen.

Door operationele redenen of onvoorziene omstandigheden kan van bovenstaande planning worden afgeweken. Voor informatie over vliegbewegingen zie www.defensie.nl/actueel/vliegbewegingen. Voor nadere vragen en eventuele klachten kan worden gebeld met staf voorlichting vliegbasis Leeuwarden 058-2346700. Voor klachten kan eveneens worden gebeld met het gratis nummer 0800-0226033.

Noot voor de redactie: Voor meer informatie kunt u contact opnemen met Staf Voorlichting vliegbasis Leeuwarden, 058-2346700.

Figure A.1: Press release by the Ministry of Defense, dated 2010, January 13, announcing the exercise on the Vliehors in the period of February 01 up to 05.

Bibliography

- Evers, L. G. (2008), The inaudible symphony: on the detection and source identification of atmospheric infrasound, Ph.D. thesis, Delft University of Technology.
- Garcés, M. A., R. A. Hansen, and K. G. Lindquist (1998), Traveltimes for infrasonic waves propagating in a stratified atmosphere, *Geoph. J. Int.*, *135*, 255–263.
- Gossard, E. E., and W. H. Hooke (1975), *Waves in the atmosphere*, Elsevier Scientific Publishing Company, Amsterdam.
- Lingevitch, J. F., C. Michael, D. Dalcio, D. Douglas, R. Joel, and S. William (2002), A wide angle and high mach number parabolic equation, *J. Acoust. Soc. Am.*, *111*, 729–734.
- Press, W. H., S. A. Teukolsky, W. T. Vetterling, and B. P. Flannery (1992), *Numerical Recipes in Fortran*, Cambridge, University Press, New York.
- Sutherland, L. C., and H. E. Bass (2004), Atmospheric absorption in the atmosphere up to 160 km, *J. Acoust. Soc. Am.*, *115*, 1012–1032.

Summary

Seismo-acoustic analysis of the infrasound events on 2010, February 03

The Seismology Division of the Koninklijk Nederlands Meteorologisch Instituut received reports of vibrations in Friesland on 2010, February 03. In order to evaluate such accounts, a seismometer network and infrasound arrays are being operated. An infrasound array on Texel (TEX) and borehole seismometer near Firdgum (FDG) appeared to have measured impulsive waveforms on that specific day. The analysis of the signals pointed to an atmospheric source near Vlieland. A military exercise was confirmed by the Ministry of Defense; a total of 12 MK-82 500 pound bombs had been thrown from F-16 fighters on the Vliehors (Vlieland).

Infrasound waves of the explosions were efficiently ducted from the Vliehors towards Friesland by a strong wind between 5 and 10 km altitude. This eastward jet stream refracted the infrasound back to earth's surface after which it was experienced as vibrations. Such wind conditions are not unique but appeared 5% of the time in a year of atmospheric specifications.

The modeling of the infrasound amplitudes for a specific source under actual wind and temperature conditions might be of help in forecasting sound pressure levels at a variety of source-receiver distances.

Samenvatting

Seismo-akoestische analyse van de infrageluid gebeurtenissen op 03 februari 2010

De afdeling Seismologie van het Koninklijk Nederlands Meteorologisch Instituut ontving meldingen van trillingen in Friesland op 03 februari 2010. Een netwerk van seismometers en infrageluid wordt beheerd om dit soort meldingen te evalueren. Een infrageluid array op Texel (TEX) en boorgat seismometer nabij Firdgum (FDG) bleken impulsvormige signalen te hebben gemeten op die dag. Uit de analyse van deze meetgegevens bleek er een bron in de atmosfeer actief te zijn geweest in de buurt van Vlieland. Het Ministerie van Defensie heeft bevestigd dat er een militaire oefening op de Vliehors (Vlieland) plaatsgevonden heeft waarbij 12 bommen (type: MK-82 500 ponders) uit F-16 straaljagers geworpen zijn.

Infrageluid van deze explosies is van de Vliehors naar Friesland gepropageerd door een sterke wind tussen de 5 en 10 km hoogte. Deze oostwaartse jetstream heeft het infrageluid teruggebogen naar het aardoppervlak waarna het als trillingen is waargenomen. Dergelijke winden zijn niet uniek maar komen 5% van de tijd voor in een jaar van atmosferische specificaties.

De amplitudes van het infrageluid kunnen gemodelleerd worden, gebruikmakend van actuele wind- en temperatuurgegevens. Dergelijke modellering kan van nut zijn om het optreden van bepaalde geluiddruk niveaus te voorspellen voor verschillende bron-ontvanger afstanden.

Acknowledgments

The author acknowledges the contribution of Drs. J.D. Assink (National Center of Physical Acoustics, University of Mississippi, USA) in the amplitude modeling with the parabolic equation (see Figure 3.4). Ko van Gend (KNMI) is thanked for his accurate analysis of the seismic recordings. The help of the Gemeente Texel with operating the Texel Infrasound Arrays is gratefully acknowledged.